Cogent Engineering

ISSN: (Print) (Online) Journal homepage: https://www.tandfonline.com/loi/oaen20

Design and simulation of a novel 3-point star rectifying antenna for RF energy harvesting at 2.4 GHz

J. O Olowoleni, C. O. A Awosope, A. U Adoghe, Okoyeigbo Obinna & Udochukwu Ebubechukwu Udo |

To cite this article: J. O Olowoleni, C. O. A Awosope, A. U Adoghe, Okoyeigbo Obinna & Udochukwu Ebubechukwu Udo | (2021) Design and simulation of a novel 3-point star rectifying antenna for RF energy harvesting at 2.4 GHz, Cogent Engineering, 8:1, 1943153, DOI: 10.1080/23311916.2021.1943153

To link to this article: https://doi.org/10.1080/23311916.2021.1943153

Published online: 27 Jul 2021.

cogent engineering

ELECTRICAL & ELECTRONIC ENGINEERING | RESEARCH ARTICLE

Design and simulation of a novel 3-point star rectifying antenna for RF energy harvesting at 2.4 GHz

J. O Olowoleni[1]*, C. O. A Awosope[2], A. U Adoghe[2], Okoyeigbo Obinna[2] and Udochukwu Ebubechukwu Udo[2]

Received: 14 March 2021
Accepted: 10 June 2021

*Corresponding author: Olowoleni J. O, Department of Electrical and Information Engineering (EIE), College of Engineering, Covenant University, Ota, Nigeria
E-mail: joseph.olowoleni@covenantuniversity.edu.ng

Reviewing editor:
Kun Chen, Wuhan University of Technology, Wuhan, CHINA

Additional information is available at the end of the article

Abstract: The rectenna as a device, is critical for achieving long-distance wireless power transfer. The centrality of this study is focused on adding to the collective knowledge of the subject matter, by providing a new perspective in terms of an alternative design for the antenna component of the rectenna. Essentially, this study features a novel "3-point star" design which was simulated in comparison with the conventional square microstrip patch antenna design. Both designs (i.e., operating at the Wi-Fi band 2.4 GHz), were assessed in terms of simulated performance parameters: gain, directivity, return loss, radiation pattern, and efficiency. From the simulation results, the proposed "3-point star" design, though slightly less efficient exhibited improved performance over the conventional square patch alternative, in terms of gain, directivity, and return loss. For the rectifying component, a greinacher voltage-doubler (with two HSMS2820 diodes), was designed separately and simulated over a range of input power levels (10dBm—34dBm), for 220-Ω, 380-Ω and 810-Ω load resistances, respectively. A maximum conversion efficiency of 88.02% was achieved at 28dBm for an 810 Ω load resistance. All design simulations were executed using Advanced Design System (ADS) software.

Subjects: Aerospace Engineering; Power & Energy; Electromagnetics & Communication

J. O Olowoleni

ABOUT THE AUTHOR

Dr. (Engr). Olowoleni J. Oluwole holds both B.Sc. and M.Sc. in Electric Drive Equipment and Process Automation of Industrial Installations and technological Complexes from Krivoy Rog Technical University, Ukraine. Presently, a Ph.D. holder in Electrical and Electronics Engineering at Covenant University, Ota. Nigeria. Engr. Olowoleni, J.O. is a lecturer 1 in the Department of Electrical and Information Engineering at Covenant University, Ota. He has taught in many areas of Electrical & Electronics Engineering, and some courses in Computer Engineering.
Dr. (Engr). Olowoleni's main research interests are in the areas of Power System Stability Control; Modelling and Optimal Sizing of An Isolated Renewable Power System: A Case Study of Covenant University. Power Systems and Electric machines.

PUBLIC INTEREST STATEMENT

For the past 40 years, wireless technology has played a critical role in knitting together the fabric of our contemporary society. From the cell phones in our pockets, to the Television (TV) remote controls in our hands; from simple e-mail exchanges to the social media chats we have with ourselves, wireless technology proves to be a necessity for driving socio-economic growth and global connectivity even across remote regions of the world.

However, it is important to understand that the idea of "Wireless" technology goes beyond just wireless transmission of data/information alone. Energy (just like data) can be transmitted wirelessly over long distance as well, and it is this idea that informs the central discussion of this paper. This paper proposes a new design for the "Rectenna" – a device which has long held the promise of enabling a wireless transfer of energy between two devices separated over a distance.

Keywords: Rectenna; 3-point star antenna; square microstrip patch antenna; Greinacher voltage doubler; HSMS2820; wireless power transmission; ADS

1. Introduction

The rectifying antenna (a.k.a. rectenna) is a highly critical technology with respect to the important role it plays in the realization of wireless power transfer via electromagnetic (EM) radiation. The rectenna, as the name suggests, is essentially an integration of an antenna and a corresponding rectifier into a single circuit for which the energy component of ambient electromagnetic signals may be captured and rectified into useable DC power for charging or powering a load device (Brown, 1984).

The following Figure 1 presents a block diagram illustration of a rectenna circuit.

The functionality of the respective components (presented in Figure 1) as they relate to the development of an efficient rectenna device is highlighted as follows:

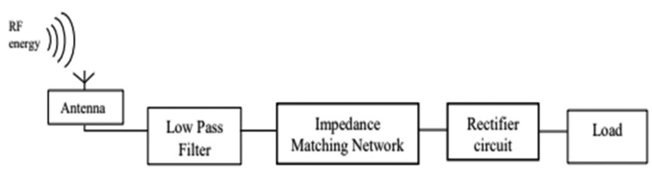

Figure 1. Block diagram of a rectenna circuit.

1.1. Antenna

The antenna is an important component in virtually all radio equipment—as it is what enables the equipment to transmit or receive electromagnetic signals between any two or more distant wireless points. In the context of signal transmission, the antenna acts as a special type of transducer which takes in an electrical signal and radiates it into space in an electromagnetic form; while in the context of signal reception, the reverse is the case, i.e. the antenna intercepts/captures ambient electromagnetic signals from which it generates electric signals at its terminals.

It is noted that two separately featured antennas in this study, were designed to function as receiver antennas to capture ambient RF signals (at 2.4 GHz) which would then be processed into useable DC power by the remaining part of the rectenna circuit. Figure 2 shows the serial configuration. Figure 3 shows the shunt configuration and Figure 4 shows the voltage doubler configuration.

The amount of power that can be received by the antenna, when it is positioned at a distance (R) from the transmitting antenna, is given by the FRIIS equation stated below.

$$P_r = P_t x\ G_t x\ G_r \left(\frac{\lambda}{4\pi R}\right)^2 \tag{1}$$

(Friis, 1946)

where,

P_t = Power of the transmitter;

G_t = Gain of transmitting antenna;

Figure 2. Serial configuration.

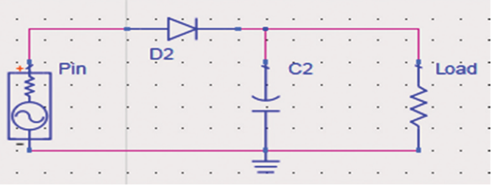

Figure 3. Shunt configuration.

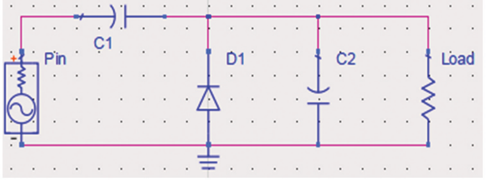

Figure 4. Voltage doubler configuration.

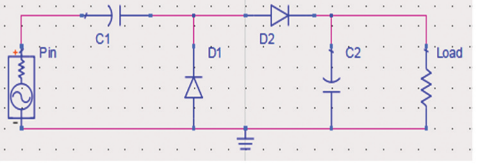

G_r = Gain of the receiving antenna;

λ = Wavelength; and

R = Distance between the transmitter and receiver.

In this study, a novel 3-point star shaped microstrip antenna design has been featured for improved performance over the conventional inset-fed square microstrip patch antenna design as shown in Figure 5.

Figure 5. Graphical illustration of a basic microstrip antenna (Sandeep & Kashyap, 2012**)**

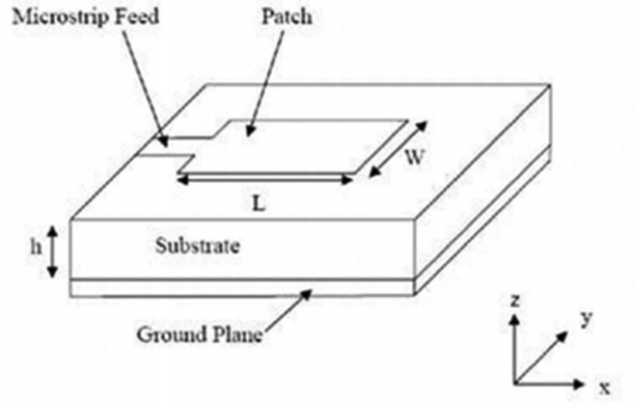

1.2. Harmonics rejection LPF

In practice, harmonics are usually generated by the rectifier components of the circuit (Roy, 2012). These generated harmonics tend to radiate back through the antenna, thereby interfering with the received electromagnetic signals.T**his** causes significant energy losses (Roy, 2012). However, these unwanted effects can be averted, or minimized with the adoption of a low pass filter (LPF) which would serve to attenuate the generated harmonics and keep them from being radiated out through the antenna (Fanga & Hassana, 2013; Han et al., 2014)

1.3. Impedance matching network

The matching network is another important part of the rectenna circuit which plays a crucial role particularly in the contest of ensuring maximum power transfer from the antenna to the load, and minimizing signal reflection. According to Jacobi's theorem (a.k.a maximum power transfer theorem), the condition for ensuring maximum power transfer to the load is that the input impedance to the load must be "conjugate matched" to the output impedance of the corresponding source (antenna) (Fotopoulou & Flynn, 2006). This is essentially where the need for a matching network comes in—as it helps in adjusting, particularly, the load impedance to ensure that it is conjugately matched to the source impedance. This serves to avert (or at least minimize) signal reflection from the load, improve the Signal-to-Noise ratio (SNR), linearize the frequency response, as well as reduce the amplitude and phase errors. All of these consequently serve to minimize signal losses and enhance the quality of power reception at the load.

1.4. Rectifier

The rectifier is another vital block of the rectenna circuit—as it is the key to ensuring an adequate RF-to-DC conversion efficiency for the circuit. Fundamentally, depending on the desired configuration, it may comprise a single or more diodes (in this case, high-frequency diodes) which serve the primary function of converting the Alternating Current (AC) signal to DC, by allowing current flow in only one direction.

With respect to available rectifier configurations, it may said that the single-diode serial and shunt rectifier configurations are generally quite popular in literature. However, with regards to generating an improved DC output voltage, the voltage multiplier configuration is taken to be more adequate—as it can potentially produce a DC output voltage that is, at least, two times the magnitude of the applied input voltage.

The following diagrams provide a schematic illustration of the three respective rectifier topologies aforementioned:

As seen in the above diagrams, the rectifier configurations differ mainly with regards to the amount and arrangement of the diodes and passive elements used. The single-diode configurations (the serial and shunt) are generally preferred in terms of their ease of implementation, small size, low cost, and high efficiency. However, their downside is revealed in the context of their low output voltage levels (Almorabeti et al., 2019). The voltage doubler topology, on the other hand, delivers a high DC voltage output, but its RF-to-DC conversion efficiency is typically less than that of the single-diode configuration.

Simulations carried out in (Hosain & Kouzani, 2013) revealed that the voltage doubler is better suited for high input power level (> 20 dB) applications, while the single-diode configurations, on the other hand, work better for low input power level (−10 dB to 20 dB) applications. Essentially, each of the rectifier topologies have their respective pros and cons. Therefore, selection of a suitable rectifier configuration generally depends on the necessary conditions, such as the size constraint, the required output voltage, and the available input power level.

1.5. Load impedance

This essentially represents the end-stage of the rectenna circuit; i.e. it represents the impedance value of the consuming device that is to be powered/charged by the rectenna. As earlier stated, to avoid signal reflections, and also obtain maximum power transfer from the antenna to the load, it is important to ensure that the load impedance is "conjugately matched" to the source impedance.

2. Related works

(Brown, 1980) provides a recollection of the early history of the development of the first rectenna device. Developed by R.H George of Purdue University, the first rectenna system was put together using an array of 28 half-wave dipole receiving antennas, each linked up to a bridge rectifier comprising four 1N82G point-contact diodes (Brown, 1984). In its early demonstration in 1964, the developed rectenna (containing 4,480 point-contact rectifier diodes) was used to power a helicopter platform for flight at about 50 feet above ground level, using beams of microwave energy at 2.45 GHz (Brown, 1996). Another early (notable) demonstration of the rectenna concept was carried out in 1975, where a successful delivery of microwave power over a distance of more than 1.6 kilometres, with over 30 kw of D.C power was obtained at the receiving end (Brown, 1996). It is reckoned that the while early innovations on the rectenna concept were focused on long distance and high-power transmissions, the more recent innovations on the rectenna seem to have been tilted towards relatively low power applications (ranging from microwatts to a few watts) delivered over moderate distances (within the range of few metres to hundreds of metres) (Clerckx et al., 2018). Table 1 below provides a highlight of some of modern state of the art rectenna designs.

3. Methodology

This section covers the design and simulation considerations for both the antenna and the accompanying rectifying circuit configuration. The configurations considered are shown in Table 1, Table 2, Table 3, and Table 4. In this study, the antenna and rectifier components of the rectenna were first

Table 1. State of the art rectennas

Ref.	Frequency	Antenna Type	Rectifier Element	Input Power	Max. η
(Niotaki et al., 2013)	915 MHz, 2.45 GHz	slot-loaded dual-band folded dipole antenna	SMS7630 Schottky diode	−9 dBm	30%, 37%
(Sun et al., 2013)	1.84 GHz, 2.14 GHz	Quasi-Yagi antenna	HSMS2852 Schottky diode	−20 dBm	34%, 30%
(Sun & Geyi, 2015)	2.45 GHz	Dual linearly polarized antenna	HSMS2860 Schottky diode	295.3 μW/cm^2	78%
(Vital et al., 2019)	2.45 GHz	Textile-based rectangular patch antenna	SMS7630 Schottky diode	8 dBm	70%
(Shi et al., 2018)	2.4 GHz	Fractal slot antenna	HSMS2852 Schottky diode	0 dBm	62%
(Agarwal et al., 2013)	2.4 GHz	Circular slotted truncated corner square patch antenna	Single-stage Dickson rectifier	0 dBm	28.9%
(Georgiadis et al., 2010)	2.45 GHz	Square aperture-coupled patch antenna	SMS7630 Schottky diode	−19.2 dBm	38.2%
(Mavaddat et al., 2014)	35 GHz	Rectangular microstrip patch antenna	MA4E1317 GaAs Schottky diode	8.45 dBm	67%
(Haboubi et al., 2014)	2.45 GHz	Cross-slot coupled square patch antenna	SMS7630-079LF diode	−15 dBm	37.7%

Table 2. Substrate parameter configuration

Parameters	Value
E_r	4.6
Freq	2.4 GHz
TanD	0.001
H	$\frac{0.0606\lambda}{E_r}$
Cond (copper)	5.8E7 S/m
T	0.7 mil

Table 3. Summary of parameter values used in the antenna design

Parameter	Square Patch Antenna Design	3-point Star Antenna Design
Substrate Material	FR4	FR4
Dielectric Constant	4.6	4.6
Substrate Height	1.6 mm	1.6 mm
Tangential Losses	0.001	0.001
Conductivity	5.8E7 S/m	5.8E7 S/m
Metal Thickness	0.7 mil	0.7 mil
Microstrip Patch Length	29.2 mm	58.4 mm
Microstrip Patch Width	29.2 mm	87.6 mm
Feedline Length (L_f)	20.2 mm	29.2 mm
Feedline Width (W_f)	3 mm	3.2 mm
Depth of Feedline (d) into the Patch	12 mm	14.6 mm
Width of the inset Gap	1.4 mm each	2.7 mm each

designed and assessed separately. The performance of the respective antenna and rectifier designs was investigated using the Advanced Design Systems (ADS) simulation software developed by Keysight Technologies.

3.1. Antenna design

While there are several antenna types available in literature, the one adopted for this study is the microstrip patch antenna for some of its apparent benefits. Microstrip antennas essentially have the benefit of being low cost, low profile, compact (and lightweight), and being conformable to both planar and non-planar surfaces. Generally, the makeup of a microstrip antenna consists of three major parts: a dielectric material (substrate), sandwiched by a metallic conducting patch (on top) and a ground plane below.

Table 4. Summary of antenna simulation results

Parameters	Square patch design	3-point star design
Frequency (GHz)	2.4 GHz	2.4 GHz
Efficiency (%)	76.9	74.8
S11 parameter (dB)	−13.6	−25.77
Gain (dBi)	5.15	6.28
Directivity (dBi)	6.29	7.54

In modelling a microstrip patch antenna, it is important to first define the antenna specifications (e.g., resonant frequency, gain, directivity, etc.) and its layer setup. The following diagram provides a graphical illustration of the makeup of a basic microstrip antenna:

Surface current is generated by the conducting patch. The dielectric substrate radiates the incident RF waves, while the ground plane acts as a reflector to help provide better directivity, by ensuring that the radiation occurs in only one direction (Das et al., 2019). The design of the microstrip antenna may be determined according to the following considerations and parameters:

(i) Dielectric Constant of the Substrate: The dielectric constant of the antenna substrate plays a defining role in determining the bandwidth, as well as the radiation efficiency of the antenna—giving it a wider impedance bandwidth, reducing the excitation of the surface wave and providing it with lower permittivity.

(ii) Thickness of Substrate Material: The thickness of the substrate has an impact on the bandwidth and coupling level. A thicker substrate provides for a wider bandwidth.

(iii) Microstrip Patch Length: The length of the microstrip patch relates to the resonant frequency of the antenna.

(iv) Microstrip Patch Width: The width of the microstrip patch is one of the important determinants of the antenna's resonant resistance. Given a wider microstrip patch, a lower resistance is obtained.

(v) Length of the Feedline: The input impedance of the antenna may be determined by the length of the feedline.

(vi) Width of Feedline: The feed line width can affect coupling to the slot as well as the return loss, and even resonant frequency.

(vii) Type of Feedline: There are several techniques that can be used to feed or transmit electromagnetic energy to the microstrip patch antenna. The feeding technique plays a critical role in improving the antenna's input impedance matching, and thus provides for an efficient operation of the antenna. Some of the different types of feeding techniques include the microstrip-line feed, inset feed, coaxial coupled feed, aperture coupled feed, and proximity coupled feed (Arora et al., 2015). It is noted that the inset feed technique was adopted in the two antenna designs evaluated in this project. The rationale behind its selection is its comparability to its alternatives, it provides the antenna with a relatively high gain, and low return loss especially when the dielectric FR4 is being used (Arora et al., 2015).

(viii) Operational Frequency: It should be noted that the operational frequency being one of the determinants of the antenna size, is a critical factor in the antenna design (Doan & Bach, 2015). More so, it is indirectly important in the context of determining the amount of available power that can be captured by the receiving antenna at a certain distance (R) from the power transmitter as given by equation 1.

Given wavelength,

$$\lambda = \frac{C}{F} \tag{2}$$

where,

C = 3 x 10^8 m/s (speed of light)

F = Operational frequency

It is seen that the wavelength (λ) of a signal is indirectly proportional to its frequency (F); thus, it may be deduced from equation 1, that the amount of power (P_r) that can be received at a certain distance from the transmitter, gets smaller as the frequency increases—given that the rise in frequency brings about a corresponding reduction in the wavelength (λ). However, frequencies within the range of 1 GHz to 3 GHz are reckoned to provide a good balance between the attenuation of power in free space and compact antenna dimensions. This paper focuses on microwave power capture and conversion at the Wi-Fi band at 2.4 GHz.

3.1.1. Substrate configuration

Table 1 shows the microstrip substrate configuration for the antenna designs including important substrate parameters values such as dielectric constant/relative permittivity “Er”, substrate thickness “H”, tangential losses “ TanD”, metal thickness “T”, conductivity “Cond”, and the operational frequency “Freq” as entered on ADS for the simulation. The structure consists of an FR4 core, with a bottom copper layer. “FR” indicates that the substrate material is flame retardant, while ‘4’ indicates that it is a woven glass reinforced epoxy resin. The FR4 board is a good general-purpose material for PCB fabrication—improving the bending and flexural strength of the antenna structure.

It should be noted that the same substrate parameter values were applied in the two antenna designs featured in this study. Also, to ensure an adequate impedance matching for the antenna, the Controlled Impedance Line Designer (CILD) tool of the ADS software was used to generate optimized values for the substrate variables to match the desired characteristic impedance of 50 ohms. After the substrate parameter values have been defined, it is also necessary to determine the basic dimensions of the inset feed patch antenna surface as shown in Figures 6 and 7.

3.1.2. Square microstrip patch antenna

The following calculations were adopted in defining the basic dimensions of the radiating surface of the antenna:

- The Width (W), and Length (L) of the radiating surface are given by:

$$W = L = \frac{c}{(2f\sqrt{\varepsilon_r})} = 29.2\ mm \quad (3)$$

where

- Speed of light, C = 3 x 10^8 m/s;
- Frequency, f = 2.4 GHz;and

Figure 6. Square microstrip patch antenna design.

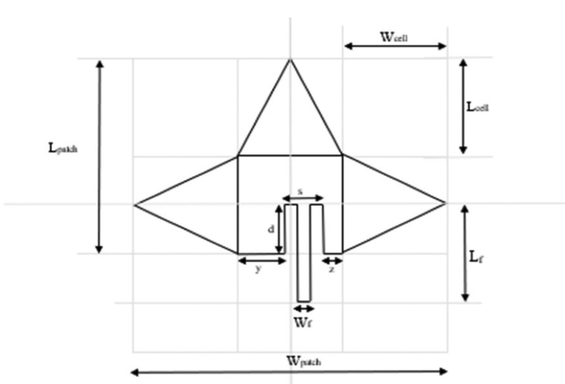

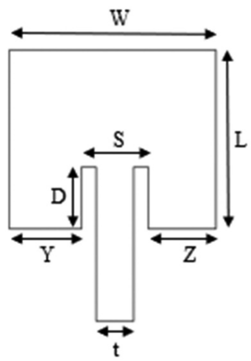

Figure 7. Proposed “3-point star” patch antenna design.

- Relative Permittivity, ε_r = 4.6

The depth of the feed line into the patch is given by:

$$\eta = \frac{P_{DC}}{P_{RF}} * 100\% \tag{4}$$

The other dimensions are given by:

$$Z \ = \ Y = \frac{2W}{5} = \frac{2x29.2}{5} = \ 11.7 \ mm \tag{5}$$

$$S \ = \ W \ - \ (Z \ + \ Y) \ = \ 5.8 \ mm \tag{6}$$

It is noted that the length and width (t) of the feed line were determined as 20.2 mm and 3 mm respectively.

3.1.3. 3-Point star microstrip patch antenna

As can be seen above, the basic “3-point star” shape is formed from a square surrounded with three equal outfacing triangles. Also, the basic dimensions of the figure can be easily determined based on the dimensions (L_{cell} x W_{cell}) of the fundamental square cells as shown above.

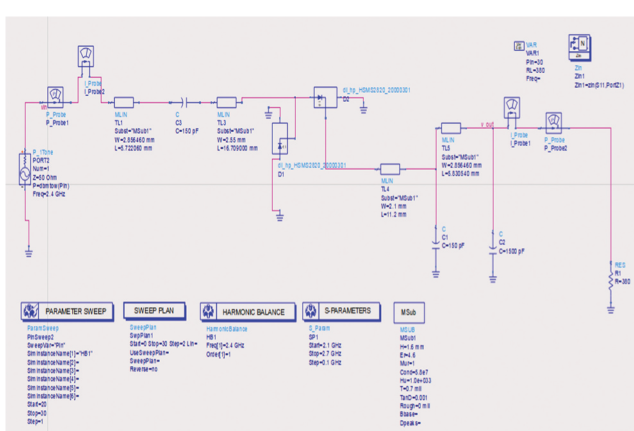

Figure 8. Schematic view of the designed rectifier circuit.

$$L_{cell} = W_{cell} = \frac{c}{(2f\sqrt{\varepsilon_r})} = 29.2\ mm \tag{7}$$

where,

- Speed of light, C = 3 × 10^8 m/s;
- Frequency, f = 2.4 GHz; and
- Relative Permittivity, ε_r = 4.6.

$$L_{patch} : W_{patch} = 2 : 3 \tag{8}$$

The depth of the feedline (d) into the patch

$$d = \frac{L_{cell}}{2} \tag{9}$$

Length of the Feedline:

$L_f = L_{cell}$ = 29.2 mm (10)

Width of the Feedline: Given some of the similarities shared with the inset-fed square patch antenna design above, the value for the width of the feedline (W_f) was initially kept constant at 3 mm, just as with the inset-fed square patch design. However, a possible mathematical relationship (yet to be conclusively proven) explaining the derivation of W_f was determined as shown in equation 11 below.

$$W_f = \frac{W_{patch}}{W_{cell}} = 3mm \tag{11}$$

However, the optimized value obtained for W_f was 3.2 mm.

Position of the feedline: it should be noted that unlike the square microstrip patch design, the position of the feedline with respect to the width of the “3-point star” patch is not centralized, but rather shifted towards the edge of the patch to an optimal position that provides for a suitable impedance matching (and return loss) with resonant frequency at 2.4 GHz. In this paper, this optimal position was painstakingly determined at first by a trial and error approach to obtain the final dimensions for y and z, which were determined to be 12.5 mm and 8.1 mm respectively. Consequently, it should be reckoned that the optimized values obtained for y and z are not presented based on any specified mathematical relationship or theoretical justification.

3.1.4. Summary of antenna design parameters

The table below provides a summary of the substrate parameters and dimension values taken into consideration for the two antenna designs.

3.2. Rectifier design

A schematic view of the final rectifying circuit is shown in Figure 8 below. The circuit which is terminated to a 380-Ω impedance, comprises two HSMS2820 diodes, Microstrip Line (MLIN) components (some of which play a role in matching the input and output impedance of the circuit), capacitors, and so on.

As with the antenna, the rectifier circuit was designed and optimized for an FR4 substrate (dielectric constant = 4.6, Substrate Height = 1.6 mm, Thickness = 0.7 mil, Tangential Losses =

0.001) using Advance Design System (ADS) simulation software. A greinacher voltage doubler configuration was adopted in the design and the conversion efficiency was simulated with respect to three different load impedances at a range of load at range of 10dBm to 34dBm of the input power. This was aided by the use of ADS parameter sweep simulation controller, alongside the harmonic balance simulation controller. Harmonic balance simulation makes it possible to simulate circuits with multiple input frequencies. It also provides for the calculation of the magnitude and phase of currents or voltage in a potentially non-linear circuit. The ADS “Line Calc” tool was used in generating optimized values for the length and width of the respective microstrip line (MLIN) components in the circuit.

4. Performance evaluation

4.1. Simulated antenna performance

As earlier stated, the featured antennas were designed to operate at 2.4 GHz. Both antenna designs were simulated and evaluated according to performance parameters such the antenna gain, directivity, return loss, radiation pattern and efficiency. A highlight of the simulation results obtained is presented as follows:

4.1.1. 3D view of the antenna designs

Figure 9 and Figure 10 show simulated 3D views of the square patch antenna as designed on ADS using the obtained dimensional parameters and substrate variables. Figure 9 presents a 3D view of the inset fed square patch antenna design (9a) and its surface current distribution at 2.4 GHz (9b). In Figure 10, the 3D view and surface current distribution (at 2.4 GHz) of the proposed 3-point star antenna design are shown.

4.1.2. S_{11} Parameter/return loss

In practice, S11 is one of the most commonly used parameters when it comes to evaluating the performance of antennas. S11 relates to the extent in which incident power would be reflected from the antenna; therefore, it may also be referred to as the reflection coefficient (or return loss), usually denoted by the Greek letter, gamma (Γ). Where S11 = 0 dB, it is interpreted that 100% of the incident power was reflected back by the antenna at its port, thus nothing was radiated. But where S11 = −13.6 dB, the implication is that if 5 dB is incident on the antenna, the magnitude of power reflected from the antenna would be −8.6 dB, while the rest would be received by the antenna. This accepted power could either be radiated or absorbed as losses within the antenna; the desired outcome, however, is that a good majority of the accepted power is radiated.

It can be seen from the figure 11 above that the square patch antenna radiates best at 2.4 GHz, where S_{11} = 13.619 dB. More so, the figure shows that at 2.1 GHz to 2.2 GHz, and further down at 2.5 GHz to 2.7 GHz, the antenna radiates virtually nothing as S_{11} approaches 0 dB. Essentially, the return loss increases as the frequency value deviates from 2.4 GHz. For the proposed 3-point star antenna design, a return loss of −25.77 dB was achieved at 2.4 GHz as shown in Figure 11.

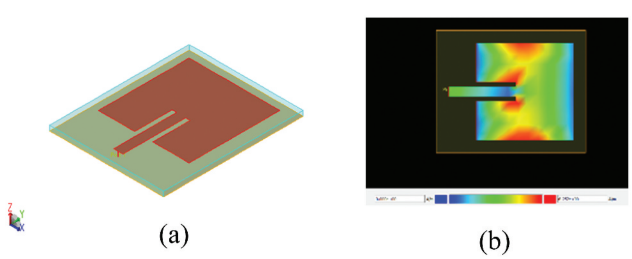

Figure 9. Simulated view of the square microstrip patch antenna.(a) 3D view (b) Surface current distribution.

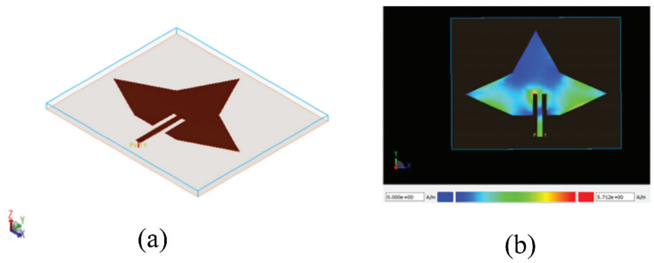

Figure 10. Simulated view of the 3-point star antenna design. (a) 3D view (b) Surface current distribution.

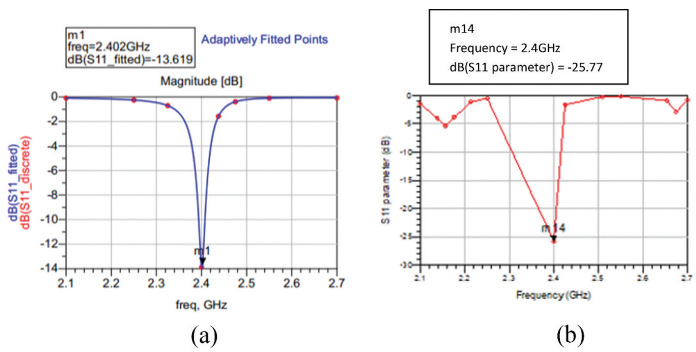

Figure 11. S11 Parameter. (a) Square patch design (b) 3-point Star design.

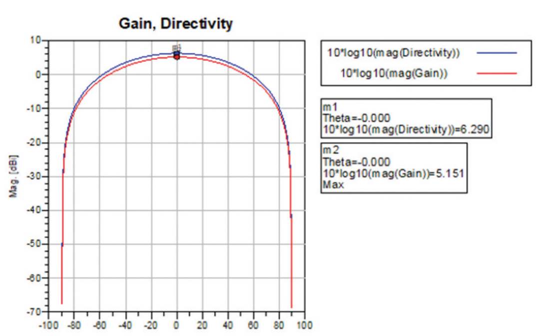

Figure 12. Combined gain and directivity plot [3-point star antenna].

4.1.3. Gain and directivity

The gain and directivity of a designed antenna are two very important antenna performance indicators, typically measured in reference to an isotropic antenna. i.e. an "ideal" antenna which receives or transmits energy uniformly in all directions. For a receiving antenna, the gain best describes the antenna's ability to capture incident radio/microwaves coming from a particular direction, in comparison to an isotropic antenna. The antenna's directivity on the other hand is a measure of the degree to which the antenna's radiation can be concentrated into a specific direction as against being uniformly spread in all directions. The simulated gain and directivity

Figure 13. Radiation pattern of square patch design.(a) Top view (b) Isometric view.

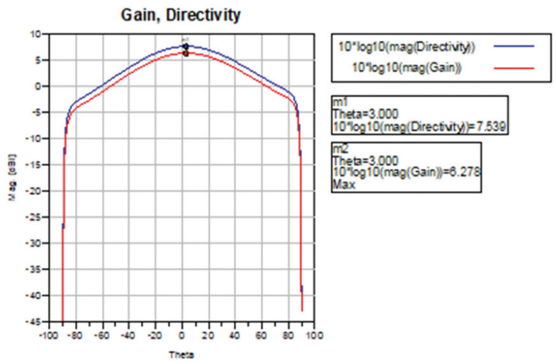

values achieved for the designed square patch microstrip antenna were 5.15101 dBi, and 6.2903 dBi respectively. However, for the proposed "3-point star" antenna design, gain and directivity values of 6.28 dBi and 7.54 dBi respectively were achieved. A combined plot of the antenna gain and directivity for the two featured antenna designs are presented in Figure 12 and Figure 13

4.1.4. Radiation pattern

In practice, energy radiated by an antenna is not uniform in all directions. The antenna's radiation is typically found to be maximum in one direction, whereas it may be minimum or near zero in other directions. The radiation pattern therefore informs on the directivity of the antenna. The following Figures 14 and 15 below show a 3D representation of the respective antenna's far-field radiation pattern. It can be seen that for both antenna designs, power would be radiated in a certain direction, thus the physical orientation of the antenna is a critical factor to be considered in its implementation as a receiver. For an effective performance, it should be positioned towards the direction of the transmitter.

4.1.5. Summary of antenna simulation results

4.2. Simulated rectifier performance

The rectifier's conversion efficiency was measured with respect to three different load impedances (220 Ω, 380 Ω, and 810 Ω) at a range of 10 dBm to 34 dBm input power level. The efficiency value is defined by the equation:

$$\eta = \frac{P_{DC}}{P_{RF}} * 100\% \tag{12}$$

Figure 14. Radiation pattern of 3-point star design.(a) Top view (b) Isometric view.

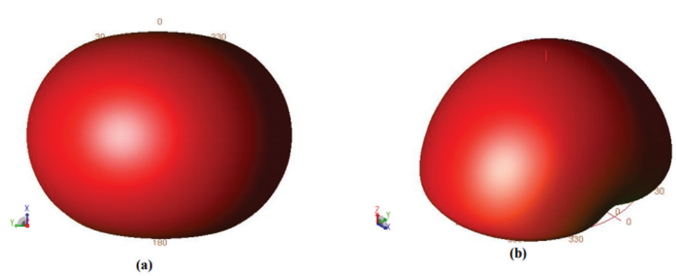

Figure 15. Plot of conversion efficiency.

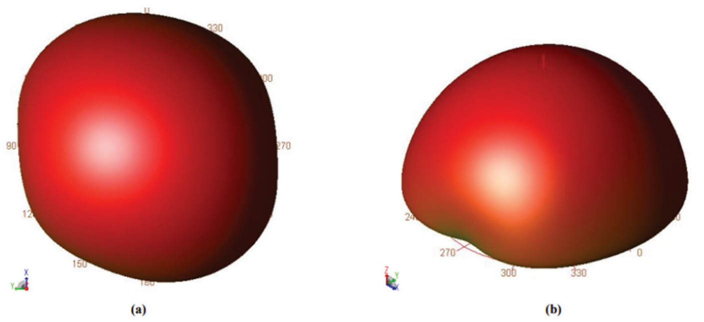

where,η = efficiency,

P_{DC} = output DC power

P_{RF} = source input RF power

In Figure 16 below, the measured efficiency values at the selected range of input power levels is plotted. The optimal load resistance (in terms of conversion efficiency) was determined to be around 810 Ω for a 28-dBm input power level at 2.4 GHz frequency.

Accordingly, the maximum conversion efficiency achieved was 88.02 % for the load impedance of 810 Ω at 28dBm. Also, as can be observed from the figure, the conversion efficiency tends to increase until the input power reaches a threshold level, where the conversion efficiency attains a peak value, and then goes on to decrease rapidly for higher power levels. Thus, it is recognized that for the proposed rectifier circuit, there is an optimal load impedance value at which a peak conversion efficiency can be achieved for a particular input power level. It is also noted that between 16dBm and 30dBm input power, the conversion efficiency exceeded 60 % for the three respective load impedances as shown above. Finally, an unimpressive return loss of −4.789 dB was recorded for the rectifier, thus reflecting the need to improve on the impedance matching of the circuit.

Figure 16. Plot of Conversion Efficiency

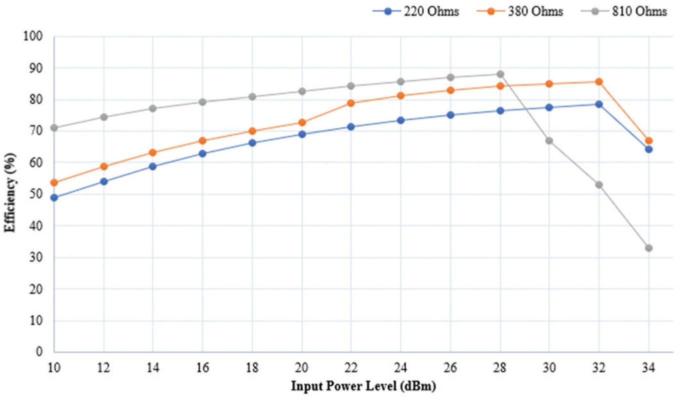

5. Conclusion

A novel 3-point star antenna design has been featured and simulated in comparison to the conventional square microstrip patch antenna design according to performance parameters such as gain, directivity, return loss, radiation pattern and efficiency. From the obtained simulation results, the proposed 3-point star antenna design was shown to exhibit improved performance over the conventional square patch antenna design in terms of gain, directivity, and return loss. However, with respect to the antenna's radiation efficiency, size (compactness) and ease of fabrication, the conventional square microstrip patch antenna design is shown to be the better alternative of the two. In view of these obtained results, in future work, the objective would be focused on improving the rectenna performance, and practically validating this design. Finally, it is worth noting that for practical implementation, the antenna and rectifier circuit can be coupled via a SubMiniature version A (SMA) connector. The SMA connector is a 50-Ohm coaxial which utilizes a screw type coupling mechanism, and can work or frequencies even as high as 17 GHz. On the other hand, the patch antenna and rectifier circuit can be directly integrated on a single substrate without the need for SMA connectors. This could serve to avert losses associated with the SMA connector, and therefore provides a higher microwave to DC conversion efficiency.

Acknowledgements
The authors wish to appreciate Covenant University Centre for Research, Innovation, and Discovery (CUCRID) for the financial support provided in the development of this study

Funding
The authors received no direct funding for this research. The authors wish to appreciate Covenant UniversityCentre for Research, Innovation, and Discovery (CUCRID) for the financial support provided in the development ofthis study.

Author details
J. O Olowoleni[1]
E-mail: joseph.olowoleni@covenantuniversity.edu.ng
ORCID ID: http://orcid.org/0000-0002-0402-0354
C. O. A Awosope[2]
A. U Adoghe[2]
Okoyeigbo Obinna[2]
Udochukwu Ebubechukwu Udo[2]
[1] Department of Electrical and Information Engineering (EIE), College of Engineering, Covenant University, Ota, Nigeria.
[2] Kanni Samah Consultants, Ilupeju, Lagos, Nigeria.

Citation information
Cite this article as: Design and simulation of a novel 3-point star rectifying antenna for RF energy harvesting at 2.4 GHz, J. O Olowoleni, C. O. A Awosope, A. U Adoghe, Okoyeigbo Obinna & Udochukwu Ebubechukwu Udo, *Cogent Engineering* (2021), 8: 1943153.

References

Agarwal, K., Mishra, T., Karim, M. F., Chuen, M. O. L., Guo, Y. X., & Panda, S. K., "Highly efficient wireless energy harvesting system using metamaterial based compact CP antenna," in *2013 IEEE MTT-S International Microwave Symposium Digest (MTT)*, 2013, pp. 1–4. https://doi.org/10.1109/mwsym.2013.6697693

Almorabeti, S., Rifi, M., & Terchoune, H. (2019). Rectifier circuit designs for rf energy harvesting applications.

Arora, A., Khemchandani, A., Rawat, Y., Singhai, S., & Chaitanya, G. (2015). Comparative study of different feeding techniques for rectangular microstrip patch antenna. *International Journal of Innovative Research in Electrical, Electronics, Instrumentation and Control Engineering*, *3* (5), 32–35. https://doi.org/10.17148/IJIREEICE.2015.3509.

Brown, W. C. (1980). The history of the development of the rectenna. *Solar Power Satellite Microwave Power Transmission and Reception*, 271.

Brown, W. C. (1984). The history of power transmission by radio waves. *IEEE Transactions on Microwave Theory and Techniques*, *32*(9), 1230–1242. https://doi.org/10.1109/TMTT.1984.1132833

Brown, W. C. (1996). The history of wireless power transmission. *Solar Energy*, *56*(1), 3–21. https://doi.org/10.1016/0038-092X(95)00080-B

Clerckx, B., Costanzo, A., Georgiadis, A., & Carvalho, N. B. (2018). Toward 1G mobile power networks: RF, signal, and system designs to make smart objects autonomous. *IEEE Microwave Magazine*, *19*(6), 69–82. https://doi.org/10.1109/MMM.2018.2844018

Das, T. T., Vinayak, S., & Pai, S. N. (2019). Design of an energy harvesting system for wireless power transmission using microstrip antenna. *Engineering Vibration, Communication and Information Processing*, *Springer*, 481–494. ed. https://doi.org/10.1007/978-981-13-1642-5_43

Doan, C. H., & Bach, D. G. (2015). Investigation of rectifier circuit configurations for microwave power transmission system operating at S Band. *International Journal of Electrical and Computer Engineering*, *5*. https://doi.org/10.11591/ijece.v5i5.pp967-974

Fanga, L. H., & Hassana, S. I. S. (2013). Comparison study on chebyshev and composite lowpass filter for harmonic rejection in two ways radio. *Procedia Engineering*, *53*, 303–311. https://doi.org/10.1016/j.proeng.2013.02.040

Fotopoulou, K., & Flynn, B. W. (2006). Wireless powering of implanted sensors using RF inductive coupling. *SENSORS*, *2006*, 765–768. *IEEE*. https://doi.org/10.1109/icsens.2007.355581

Friis, H. T. (1946). A note on a simple transmission formula. *Proceedings of the IRE*, *34*(5), 254–256. https://doi.org/10.1109/JRPROC.1946.234568

Georgiadis, A., Andia, G. V., & Collado, A. (2010). Rectenna design and optimization using reciprocity theory and harmonic balance analysis for electromagnetic (EM) energy harvesting. *IEEE Antennas and Wireless Propagation Letters*, *9*, 444–446. https://doi.org/10.1109/LAWP.2010.2050131

Haboubi, W., Takhedmit, H., Luk, J.-D. L. S., Adami, S.-E., Allard, B., Costa, F., Vollaire, C., Picon, O., & Cirio, L. (2014). An efficient dual-circularly polarized rectenna for RF energy harvesting in the 2.45 GHz ISM band. *Progress In Electromagnetics*

Research, *148*, 31–39. https://doi.org/10.2528/PIER14031103

Han, M., Jung, S., & Sohn, H., "High efficient rectenna using a harmonic rejection low pass filter for RF based wireless power transmission," in *2014 11th International Symposium on Wireless Communications Systems (ISWCS)*, 2014, pp. 423–426. https://doi.org/10.1109/iswcs.2014.6933390

Hosain, M. K., & Kouzani, A. Z., "Design and analysis of efficient rectifiers for wireless power harvesting in DBS devices," in *2013 IEEE 8th Conference on Industrial Electronics and Applications (ICIEA)*, 2013, pp. 651–655. https://doi.org/10.1109/iciea.2013.6566448

Mavaddat, A., Armaki, S. H. M., & Erfanian, A. R. (2014). Millimeter-wave energy harvesting using microstrip patch antenna array. *IEEE Antennas and Wireless Propagation Letters*, *14*, 515–518. https://doi.org/10.1109/LAWP.2014.2370103

Niotaki, K., Kim, S., Jeong, S., Collado, A., Georgiadis, A., & Tentzeris, M. M. (2013). A compact dual-band rectenna using slot-loaded dual band folded dipole antenna. *IEEE Antennas and Wireless Propagation Letters*, *12*, 1634–1637. https://doi.org/10.1109/LAWP.2013.2294200

Roy, S. (2012). *Designing of a small wearable conformal phased array antenna for wireless communications*. North Dakota State University.

Sandeep, B. S., & Kashyap, S. S. (2012). Design and simulation of microstrip patch array antenna for wireless communications at 2.4 GHz. *International Journal of Scientific & Engineering Research*, *3*, 1–5.

Shi, Y., Jing, J., Fan, Y., Yang, L., Li, Y., & Wang, M. (2018). A novel compact broadband rectenna for ambient RF energy harvesting. *AEU - International Journal of Electronics and Communications*, *95*, 264–270. https://doi.org/10.1016/j.aeue.2018.08.035

Sun, H., & Geyi, W. (2015). A new rectenna with all-polarization-receiving capability for wireless power transmission. *IEEE Antennas and Wireless Propagation Letters*, *15*, 814–817. https://doi.org/10.1109/LAWP.2015.2476345

Sun, H., Guo, Y.-X., He, M., & Zhong, Z. (2013). A dual-band rectenna using broadband Yagi antenna array for ambient RF power harvesting. *IEEE Antennas and Wireless Propagation Letters*, *12*, 918–921. https://doi.org/10.1109/LAWP.2013.2272873

Vital, D., Bhardwaj, S., & Volakis, J. L., "A 2.45 GHz RF power harvesting system using textile-based single-diode rectennas," in *IEEE MTT-S International Microwave Symposium Digest*, 2019, pp. 1313–1315. https://doi.org/10.1109/mwsym.2019.8700836